

# Diagonal Tension Field Inclination Angle in Steel Plate Shear Walls

Yushan Fu<sup>1</sup>; Fangbo Wang<sup>2</sup>; and Michel Bruneau, F.ASCE<sup>3</sup>

**Abstract:** Research was conducted to investigate how the inclination angle of the diagonal tension field action varies in steel plate shear walls (SPSWs) and to determine what optimum constant angle best matches the demands obtained from finite-element (FE) analysis. An FE model was first calibrated against experimental results that surveyed inclination angles across the web plate of an idealized SPSW as a function of drift and that showed significant differences in inclination angles at different locations across the web plate. Then, four real SPSWs with varying aspect ratios and numbers of stories were designed and modeled for FE analyses. The variations in angle in the web plate and along the boundary elements were documented as a function of drift and showed significant variations. Combined moment–axial force demand ratios in the SPSW boundary elements were calculated and compared for all real SPSWs to determine the preferable value of single angle that could be used in design. Overall, using 45° was found to be a reasonable compromise for both horizontal and vertical boundary element (HBE and VBE, respectively) design if a single constant angle is desired. Furthermore, the demand on the web plate is not sensitive to the variation of inclination angle. Consequently, the single angle of 45° is recommended for the design of the entire SPSW. DOI: 10.1061/(ASCE)ST.1943-541X.0001779. © 2017 American Society of Civil Engineers.

**Author keywords:** Steel; Plate; Shear; Wall; Inclination angle; Tension; Field; *LS-DYNA*; Seismic effects.

## Introduction

A typical steel plate shear wall (SPSW) consists of horizontal boundary elements (HBEs), vertical boundary elements (VBEs), and web plates. The ultimate strength of SPSWs is reached when the web yield in diagonal tension-field action at an angle  $\alpha$  from the vertical and HBEs develop plastic hinging at their ends. Capacity design of a SPSW requires the web plate to have sufficient strength to resist the specified story shear, and the HBE and VBE to be able to resist the diagonal forces applied by the web plate on those boundary elements. Therefore, the inclination angle, denoted as  $\alpha$ , is a key parameter in SPSW design. AISC 341-10 (AISC 2010) provides an equation to calculate the inclination angle [based on research by Timler and Kulak (1983)]. Although this approach is generally accepted in design practice, this angle  $\alpha$  was derived from an elastic strain energy principle, whereas seismic design usually expects structures to develop plastic behavior. Alternatively, for simplicity, AISC 341-10 also allows using a constant angle of 40° based on work by Dastfan and Driver (2008).

Researchers have observed from experimental or numerical results that the inclination angle typically varies between 38° and 45° for well-designed SPSWs. The quasi-static experiment conducted by Timler and Kulak (1983) showed that the angle of inclination

along the vertical centerline of the web plate varied from 44° to 56°. Elgaaly et al. (1993) performed finite-element analysis using shell elements and reported that the principal tension stress direction in the central area of the plate panel varied between 40° and 50°. In Driver et al. (1997), the principal stress directions derived from the strain rosette data near the top right corner of a web plate varied from 38° to 64°, compared with the finite-element results varying from 35° to 65°. Lubell (1997) plotted the principal tension strains along the boundary elements and the center of the panel plate at angles of inclination from the vertical, most of which were in the range of 35–40°. In Rezaei's (1999) shake table test of a steel plate shear wall with thin unstiffened webs, strain rosette results showed that the angle of principal strain varied from 35° to 40° near the base, and from 37° to 42° at the center of the panel. Kharrazi (2005) measured the angle of tension field at the crest of the buckle wave from a test, which ranged from 37° to 39°, and compared those to the in-plane principal stress vectors obtained from FE analyses, which were in a similar range of 34°–40°. Choi et al. (2009) used *ABAQUS* to perform a parametric study of the inclination angle under different aspect ratios, infill plate thicknesses, and endplate thicknesses, which showed that the average inclination angle of the tension field in the yielded web varied from 24° to 45°. More recently, Webster et al. (2014) conducted experimental investigations and finite-element analyses studying how the inclination angle changes as a function of drift. In particular, two specimens with pin connection and slender VBE were tested, and the experimental results agreed well with results from FE analysis (conducted with *ABAQUS*). The inclination angles, both calculated by averaging values over the whole web and by measuring the orientation of the buckled corrugations, were different from the value predicted by AISC (2010). Because the average inclination angle of single panels fixed within an elastic boundary frame at the typical design seismic drifts varied between 43° and 45°, and because a constant angle of 45° was believed to be simpler to implement, Webster et al. (2014) recommended using a constant angle of 45° for both capacity design procedure and cyclic analysis of the SPSW system. However, the specimens considered by Webster had essentially rigid

<sup>1</sup>Graduate Research Assistant, Dept. of Civil, Structural and Environmental Engineering, Univ. at Buffalo, Amherst, NY 14260 (corresponding author). ORCID: <http://orcid.org/0000-0003-3258-3389>. E-mail: yushanfu@buffalo.edu

<sup>2</sup>Graduate Research Assistant, Dept. of Civil, Structural and Environmental Engineering, Univ. at Buffalo, Amherst, NY 14260. E-mail: fangbowa@buffalo.edu

<sup>3</sup>Professor, Dept. of Civil, Structural and Environmental Engineering, Univ. at Buffalo, Amherst, NY 14260. E-mail: bruneau@buffalo.edu

Note. This manuscript was submitted on July 8, 2016; approved on December 15, 2016; published online on March 15, 2017. Discussion period open until August 15, 2017; separate discussions must be submitted for individual papers. This paper is part of the *Journal of Structural Engineering*, © ASCE, ISSN 0733-9445.

HBEs, slender VBEs, and pure pin connections between the boundary frame members, for the sake of experimental purposes, which made them different from real SPSWs. Although consideration of a single angle of  $45^\circ$  is appealing for design purposes, it is unknown whether the findings reported by Webster et al. (2014) would remain true for real SPSWs with realistic boundary elements, different aspect ratios, and different numbers of stories. Such information is required to overcome possible (and arguably, founded) reservations from code committee members against changing the design requirements for SPSWs. Furthermore, because the forces induced to the HBEs and VBEs by the yielding web are directly related to the inclination angle developed near the boundary elements, additional detailed information of the angle along such boundary element, and information on how these demands compare to those obtained using a constant inclination angle, is also required.

The work reported in this study was conducted to expand on prior knowledge and provide the additional evidence needed to determine what should be the optimum inclination angle of the tension field action to consider for the design of SPSWs. Furthermore, in the process of investigating how the inclination angle of the diagonal tension field action varies in different locations of SPSWs, particular attention was paid to determine the demands from these angles on the boundary elements and the effect and impact of these angles on the design of both the web and the boundary elements (HBEs and VBEs). Finally, based on all these results for all components of the SPSWs, the objective of this research was to determine what the optimum constant angle to use for the design of SPSWs best matches the demands obtained from finite-element analysis. In simpler terms, the research investigated how the inclination angle of the tension field action changes in real SPSWs having different aspect ratios and numbers of stories, at various drifts through nonlinear inelastic response for SPSWs designed in compliance with AISC (2010), and how this change impacts design. Ultimately, the objective was to determine whether the constant inclination angle of  $40^\circ$  provided in the AISC Seismic Specifications should continue to be used, or whether it should be replaced by a different value, such as the  $45^\circ$  value recommended by Webster et al. (2014) or any other value.

The investigation was conducted using the *LS-DYNA* finite-element software to model SPSWs. The *LS-DYNA* model was first calibrated by replicating the experimental and *ABAQUS* analysis results obtained by Webster et al. (2014) for simple tested specimens having pin HBE-to-VBE connections and cutouts at the web plate corners. Then, this validated *LS-DYNA* finite-element model was used to further investigate the changes in inclination angle and their impact on SPSW behavior for modified versions of Webster's specimen, first without cutouts at the corner of the webs, and then with rigid HBE-to-VBE connections (still without the web cutouts).

Then, two real single-story SPSWs and two real 3-story SPSWs were subsequently designed, with panel aspect ratios of 1 and 2. Corresponding *LS-DYNA* models were built also modeling the HBEs and VBEs. The plastic behavior of HBE was captured by considering development of the plastic hinge at the end of the HBEs. This was done to observe how the inclination angle varied as a function of number of stories and panel aspect ratios for SPSWs designed per AISC (2010). To determine what appropriate or optimum constant angle should be used for SPSW design, demands from actual results obtained from finite-element analysis, and demands calculated using various assumed constant inclination angles, were compared for all cases of SPSWs aspect ratio and number of stories considered. For HBEs and VBEs, these were expressed by calculating combined moment–axial force demand ratios. In this paper, the terms HBE and beam, as well as VBE and column, are used interchangeably, because both terms are commonly used in the literature.

## Model Calibration

### Dimensions and Boundary Conditions

In the *LS-DYNA* model developed to replicate Specimen 2-22 in Webster et al. (2014), dimension of the steel web plate is  $762 \times 762 \times 0.71$  mm (length  $\times$  height  $\times$  thickness). Width of the cutout in each corner of the web plate is 140 mm. The VBE is a  $25.4 \times 63.5$  mm rectangular section. The HBE is a  $71 \times 150$  mm rectangular section, made equivalent to the  $W6 \times 25$  section used in Webster et al. (2014) by having the same depth and moment of inertia. Connection between the VBE and HBE in the Webster et al. (2014) specimen was achieved by using an actual pin, and a point connection was implemented in the *LS-DYNA* model to achieve the same behavior. The bottom beam was continuously fixed along the wall's base. To account for initial imperfections, the nodes in the web plate were initially perturbed using a harmonic field with an amplitude of  $t/2 = 0.035$  mm in the  $z$ -direction (i.e., perpendicular to the plate) and a wavelength of 1524 mm in both  $x$ - and  $y$ -directions.

### Material and Element

The constitutive model chosen for the steel web plate was an elastic-plastic model without strain rate effect. (i.e., material MAT024\_PIECEWISE\_LINEAR\_PLASTICITY in *LS-DYNA*). The material was specified in this study as having a Young's modulus of 151,000 MPa, a yielding strength of 287 MPa, a Poisson ratio of 0.30, and a density of  $7,850$  kg/m<sup>3</sup>. Because they were reported to remain elastic in the Webster et al. (2014) study, beams and columns were modeled as an elastic material (i.e., using *LS-DYNA*'s material MAT001\_ELASTIC), with a Young's modulus of 205,000 MPa and a Poisson ratio of 0.30 [all aforementioned numerical values were taken as those reported by Webster et al. (2014)]. To model the actual pin joint of the beam-column connection, beam and column elements in the overlapping area were modeled with separate and independent finite-element meshes using rigid material (i.e., using *LS-DYNA*'s material MAT020\_RIGID and a Young's modulus 205,000 MPa); hence, they did not share nodes in the same location. The option JOINT\_SPHERICAL in *LS-DYNA* was used at the two center nodes (from the beam and column, respectively) in the overlapping area. The SPHERICAL JOINT option in *LS-DYNA* allows six degrees of freedoms. Only the out-of-plane degree of freedom (i.e.,  $z$ -translation) was constrained on the peripheral nodes of the overlapping area as shown in Fig. 1. Belytschko-Tsay shell elements were used for the web plate, VBEs and HBEs because of their computational efficiency. The number of through thickness integration points was set to 9, to be the same as in Webster (2013).

### Loading Protocol

A quasi-static displacement loading history was applied to each node along the middle height of the top beam. Both monotonic loading and cyclic loading scenarios were used (Fig. 2). The cyclic loading scenario applied was the same as Webster (2013). The monotonic loading scenario was used for inclination angle analyses.

### Convergence Study

To investigate convergence of results obtained from the *LS-DYNA*, a coarse mesh configuration considered provided a  $34 \times 34$  elements web plate (mesh size  $22 \times 22$  mm), whereas a refined mesh configuration was  $68 \times 68$  elements (mesh size  $11 \times 11$  mm) (Fig. 3). Both cyclic and monotonic displacement histories were

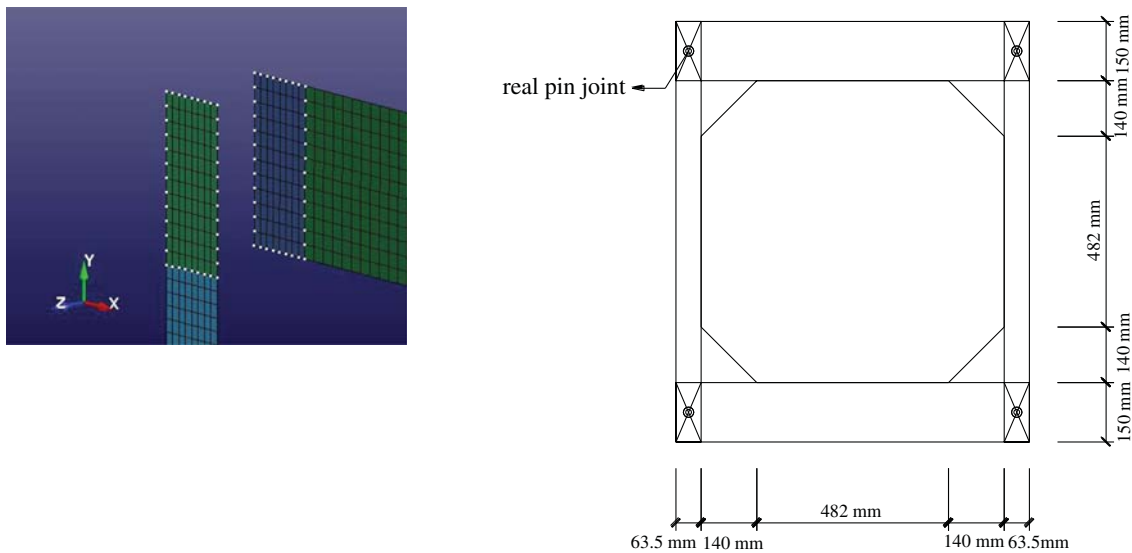


**Fig. 1.** Dimensions of the SPSW model and  $z$ -translational constrains in a beam-to-column joint

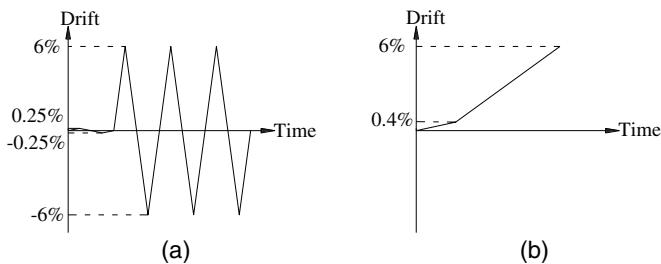


**Fig. 2.** Loading protocol: (a) cyclic loading; (b) monotonic loading

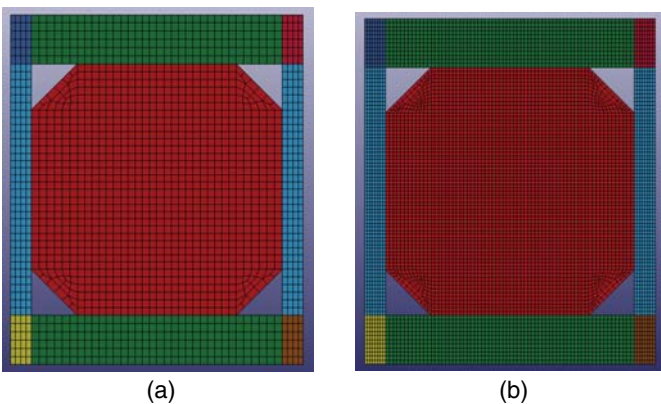


**Fig. 3.** Coarse and refined mesh used in *LS-DYNA* models: (a) coarse mesh; (b) refined mesh

used to obtain load-versus-drift relationships for the two different mesh sizes considered. *LS-DYNA*'s implicit analysis with single precision executable was adopted to analyze the model because of computational efficiency, but results obtained using *LS-DYNA*'s explicit analysis are also presented for comparison. In all implicit analyses (cyclic and monotonic), the analysis time step was 0.001 s, with termination of the analysis at a time of 8.0 s (i.e., after 8,000 steps).

The load-versus-drift curves under cyclic loading were compared with Webster's (2014) experimental and *ABAQUS* model results for validation of the model. The load-drift hysteretic curves obtained are similar to each other [Fig. 4(a)]. Peak load difference under the first 6% drift loading cycle is approximately 5 kN, and structural stiffness is slightly smaller than for the *ABAQUS* model and experimental results. Overall, the results shown in Fig. 4(a) were deemed to be in good agreement, and the *LS-DYNA* model was judged appropriate to predict structural behavior of the system.

Results obtained comparing the *LS-DYNA* coarse mesh and *LS-DYNA* refined mesh results obtained using the implicit analysis with single precision executable were in good agreement. Peak load in the first 6% drift loading cycle is 72.27 kN with coarse mesh and 70.80 kN with refined mesh, respectively. The difference is only 1.47 kN and 2.08% of the peak load with refined mesh. Additionally, comparing results obtained from the implicit and explicit solvers, the load-drift curves had negligible differences.

The average inclination angle across the entire plate was also calculated for comparison with Webster (2013), in which the mean in-plane stresses of the entire web plate (consisting of  $35 \times 35 = 1,225$  elements in total) were used. Results shown in Fig. 4(b) suggest that the maximum difference between these two curves is within  $2^\circ$ , which means that the average inclination angle across the entire plate obtained from the *LS-DYNA* model matches well with the Webster's (2014) experiment and modeling results.

### Inclination Angle Analysis

In this study, principal stress angles were averaged by outputting the in-plane stresses and calculating the inclination angle per element considered, then obtaining the average angles for each locations that have an impact on design [Fig. 5(a)]. First, with respect to the web plate, the average for all web shell elements at midheight of the wall are calculated, because this is deemed representative of the angle that should be taken to calculate the story shear force resisted by the infill plate [per AISC (2010) design equation]. Furthermore, because this is significant for the design of VBEs and HBEs, the averages of the web shell elements connected along individual VBEs and HBEs are calculated. This approach is believed to

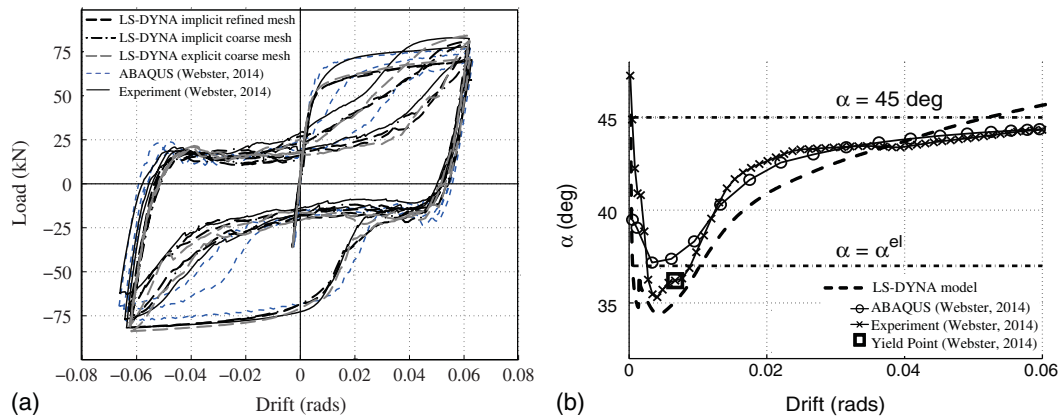


**Fig. 4.** Comparison of *LS-DYNA* and *ABAQUS* models and experimental data in Webster et al. (2014): (a) load-drift curves under cyclic loading; (b) average inclination angles over the entire web plate

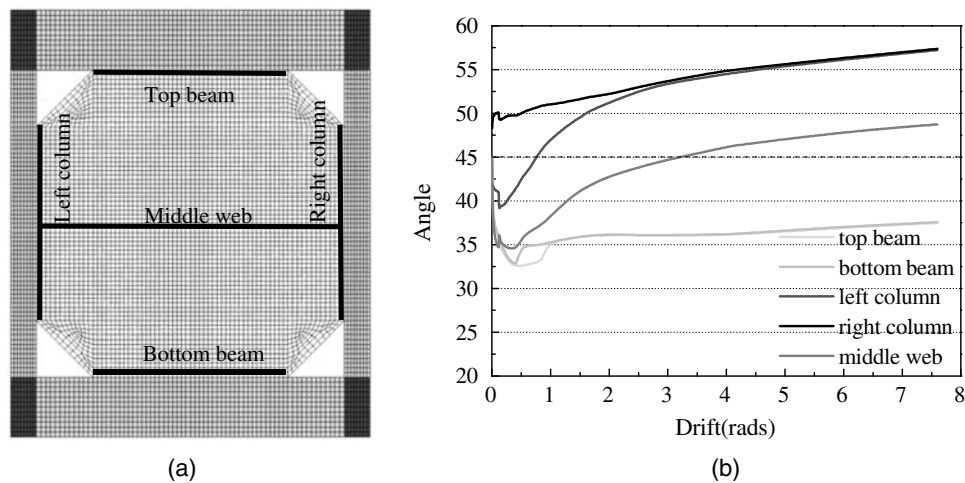


**Fig. 5.** Inclination angle variation: (a) location of shell element groups; (b) migration of inclination angle of the web plate

provide a better understanding on the design consequence of varying inclination angles.

Fig. 5(b) shows the inclination angle versus drift relationship of the web plate shell elements located along the top beam, bottom beam, left column, right column, and middle web, identified by the lines in Fig. 5(a). The angles presented in Fig. 5(b) are the averages for all the elements along each line considered.

In Fig. 5(b), all the curves exhibit a similar trend, in that the angle initially decreases from a relatively high initial value at low drift (and thus low stresses), up to nearly 0.5% drift (at which some parts of the infill approach their elastic limit), and then progressively increase afterward up to the maximum drift considered. In the earlier stages of elastic response, stresses applied by the steel plate to the boundary elements are not of design concern because the stresses are low (Fu et al. 2017). Hence, the high values of angle initially observed from 0 to 0.5% drift have no significance on structural design.

However, in spite of this similarity in trend observed in Fig. 5(b), quite different angle values are obtained along the different locations considered. Top and bottom beams have approximately the same angle values, starting as low as 33° at 0.5% drift and reaching an angle of approximately 37° beyond 3% drift. Similarly, the left and right columns have approximately the same angle values, starting as low as 40° for the left column and 50° for the right column at 1% drift, and reaching an angle of approximately

53° at 3% drift. In addition, the angle across the middle web is approximately 37° at 1% drift, 44° at 3% drift, and 48° at 6% drift.

### Effect of Cutout Corners and Beam-to-Column Connections

To investigate how the presented cutout corners and the type of beam-to-column connections affect the preceding observation that the inclination angle of the diagonal tension field action varies across the web plate, two alternative models were designed with the same material models, loading protocol, and boundary conditions as the validated *LS-DYNA* model. The main differences from the validated *LS-DYNA* model were connection type and absence of cutout. Model A is with pin HBE-to-VBE connections and without web cutouts at the corner of the web plate, and Model B is with rigid HBE-to-VBE connections and also without cutouts. In addition, elastoplastic behaviors of HBES and VBES were considered in Model B. A summary of these differences is presented in Table 1. To simulate the rigid connection of HBE and VBE, nodes at the end of the HBE were merged to the face of VBE.

Fig. 6 shows the change in inclination angle of the tension field action as a function of drift for the web plate in the three models listed in Table 1. For Model A, the angle in each location follows a similar trend as the validated model after 2% drift. Up to the

**Table 1.** Differences of the Three *LS-DYNA* Models

Differences	Validated LS-DYNA model	Model A	Model B
Connection type for HBE to VBE	Pin	Pin	Rigid
Geometry of the web plate	With cutout	Without cutout	Without cutout
Material model of VBEs and HBEs	Elastic	Elastic	Elastic-plastic

maximum drift considered, the average angles are approximately 55, 39, and 48° for VBE, HBE, and the web plate, respectively. The average angle along the right column initially increases to nearly 55° and drops after 0.5% drift, mainly because of localized angle variation at the top and bottom corners of the web, but the amplitude of stress in those corners is not large at those small drifts. For Model B, the variations in average inclination angle are similar as for the validated *LS-DYNA* models and Model A. However, the inclination angle along the left and right columns only increased to approximately 50° (as opposed to 55°) at large drifts.

## Inclination Angle for Real SPSW

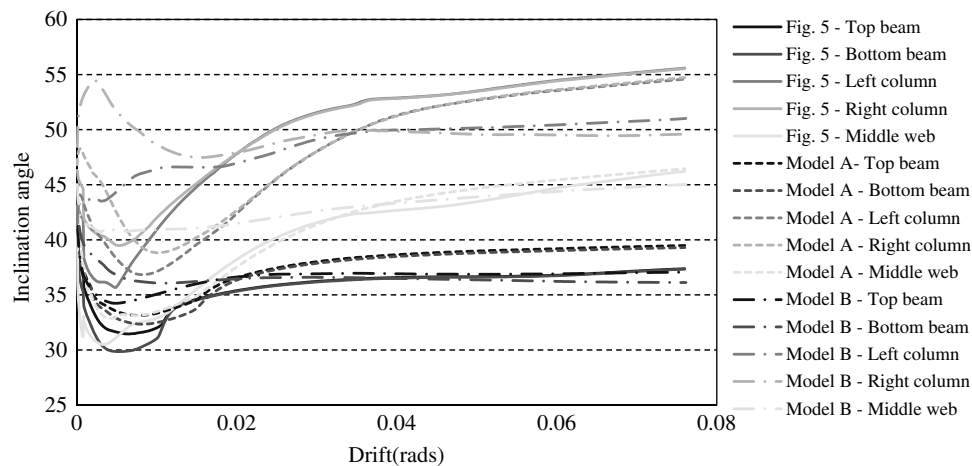
### Design of the New Real SPSWs

To broaden the previous findings and study how the inclination angle varies for SPSWs having different numbers of stories and

aspect ratios, four real SPSWs were designed to have one bay width, 3.048 m (10 ft) story height, and an aspect ratio of either 1.0 or 2.0, namely two single story SPSWs (SW11 and SW12), and two 3-story SPSWs (SW31 and SW32). For simplicity, following the example provided in Purba and Bruneau (2010), irrespective of the aspect ratio, the 3-story SPSWs were subjected to the same lateral load as the archetype SW320 described in that example, whereas the 1-story SPSWs were then taken to have the same load as that of the third floor in that example.

For the designs considered in this study, the yield strength of web plate and boundary elements were taken as 206.7 and 344.5 MPa, respectively. The required web plate thickness to resist story shear forces was determined per the AISC seismic provision (AISC 2010). No strength resistance factor was considered and the plate thickness calculated to resist 100% of the story shear force was used in subsequent calculations (instead of using actual available plate sizes), so as to not introduce overstrength in the boundary element design. The web plate yield forces, applied to their boundary elements per capacity design principles, produced axial forces, shear forces, and moments on the VBEs and HBEs (Table 2).

Although the design of HBE and VBE sections in SPSWs would normally be accomplished by selecting the lightest members that satisfy demand-to-capacity ratio less than 1.0, in this study to minimize overstrength of the boundary elements, members chosen were those that had demand-to-capacity ratio as close as possible to 1.0 without exceeding it. Because the axial force in HBE was not significant in this case, only the moment demand-to-capacity ratio was considered. The desired yielding mechanism of an SPSW entails yielding of the webs in shear followed by plastic hinging at

**Fig. 6.** Comparison of inclination angle migration of the web plate**Table 2.** Distributed Loads from the Yield Web Plate

SPSW	Story	Angle (degrees)	$t_w$ [cm (in.)]	$\omega_{xbi}$ [kN/m (kip/in.)]	$\omega_{ybi}$ [kN/m (kip/in.)]	$\omega_{xci}$ [kN/m (kip/in.)]	$\omega_{yci}$ [kN/m (kip/in.)]
SW11	1	42.25	0.180 (0.071)	183.64 (1.0488)	218.86 (1.2499)	154.11 (0.8801)	183.64 (1.0488)
SW12	1	44.57	0.091 (0.036)	93.12 (0.5318)	110.98 (0.6338)	78.13 (0.4462)	93.12 (0.5318)
SW31	3	42.45	0.180 (0.071)	183.64 (1.0488)	218.86 (1.2499)	154.11 (0.8801)	183.64 (1.0488)
	2	40.79	0.292 (0.115)	297.46 (1.6988)	354.49 (2.0245)	249.61 (1.4255)	397.46 (1.6988)
SW32	1	39.25	0.358 (0.141)	364.72 (2.0829)	434.65 (2.4823)	306.02 (1.7477)	364.72 (2.0829)
	3	44.31	0.091 (0.036)	95.67 (0.5464)	98.02 (0.5598)	93.40 (0.5334)	95.67 (0.5464)
	2	43.77	0.150 (0.059)	155.45 (0.8878)	162.27 (0.9267)	148.92 (0.8505)	155.45 (0.8878)
	1	43.89	0.182 (0.072)	188.97 (1.0792)	196.41 (1.1217)	181.81 (1.0383)	188.97 (1.0792)

Note:  $t_w$  = thickness of web plate;  $\omega_{xbi}$ ,  $\omega_{ybi}$  = distributed loads applied to the HBEs from the web plate yielding at the  $i$ th story;  $\omega_{xci}$ ,  $\omega_{yci}$  = distributed loads applied to the VBEs from the web plate yielding at the  $i$ th story.

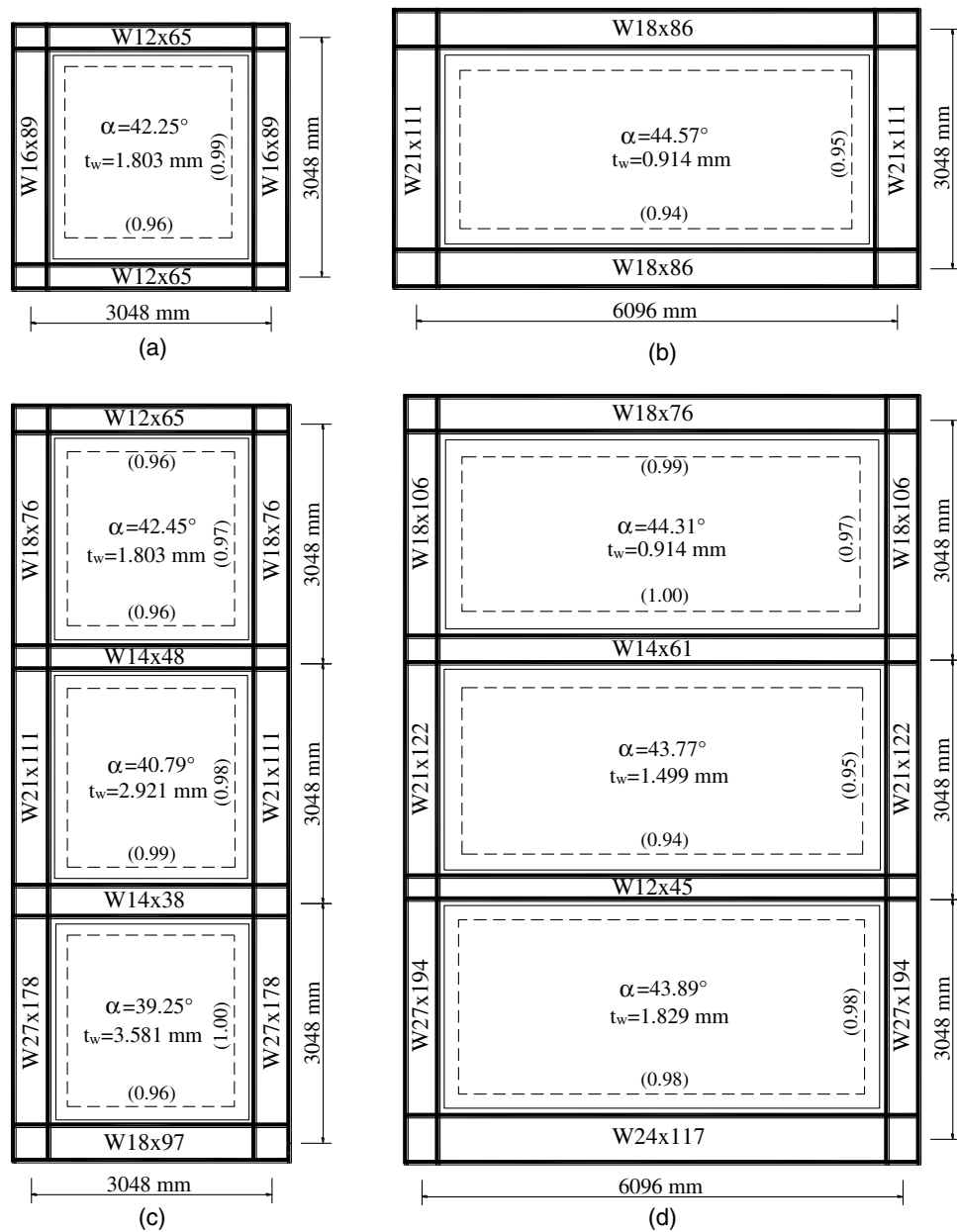


Fig. 7. SPSW elevations: (a) SW11; (b) SW12; (c) SW31; (d) SW32

the ends of the HBEs, and the resulted designs in this study are expected to similarly behave when pushed over. The resulting designed SPSWs are presented in Fig. 7.

### LS-DYNA Modeling of Four Real SPSWs

New *LS-DYNA* models were built for the four real SPSWs. Different from the validated model, the new models had three-dimensional boundary elements, which is more representative of real SPSWs. The HBEs were rigidly connected with the VBEs by merging the nodes at the same coordinate. All panel zones were defined as rigid body with respect to a nodal point at their mass centers. The nodal points of the two bottom panel zones were pin-supported on the ground by using the NODAL RIGID BODY and BOUNDARY\_PRESCRIBED MOTION RIGID. BOUNDARY\_PRESCRIBED MOTION RIGID was defined with a zero-valued load curve for all translational degrees of freedom, so that the panel zone could only rotate with respect to this point. In addition,

$z$ -constraints ( $z$  is in the direction normal to the web plate) were applied to the flange plate edge nodes of the upper panel zones, to constrain the SPSW to move within  $x$ - $y$  plane. In addition, the HBE ends, over a length equal to approximately one-sixth of the span length, were modeled with a more refined mesh to better capture the nonlinear inelastic behavior of the plastic hinges at those locations. The material model used for real SPSWs was obtained from the coupon test in Webster et al. (2014) and converted into normalized values (Fig. 8).

Node merging requires nodes from one part to share identical coordinates with those of another part. However, in this case, different flange widths of VBEs and HBEs resulted in different meshes [Fig. 9(a), arrows]. To simplify the modeling and avoid iterations of mesh size, the actual cross sections were converted into equivalent cross sections over the 3-story SPSW models. Two principles were followed for that purpose: (1) for the VBEs, the equivalent section was sized to have identical height, shear, and moment capacity as the original section, to avoid the premature yielding of the web by

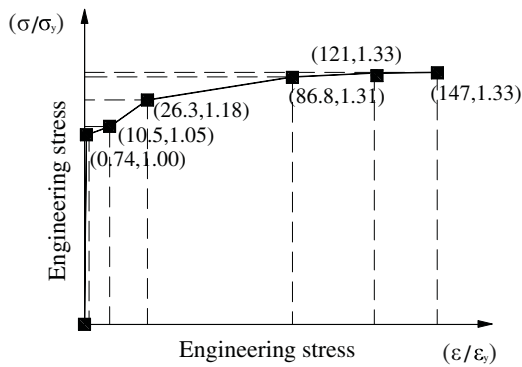


Fig. 8. Normalized material model used by Webster et al. (2014)

shear; and (2) the flange width of HBEs was converted to align with the mesh of VBEs, without changing their flange area.

Four real SPSWs were studied under monotonic loading. For SW11, both force control and displacement control were done for comparison. In the former case, a load was applied to each node along the middle height of the top beam; whereas for the latter, the displacement of the nodal point in the upper right panel zone was controlled. Conceptually, the displacement control analysis could be thought of as preventing the development of axial deformations in the top beam and possibly constraining or affecting the strain field in the web panel. However, comparison of stress results as well as moment and axial force diagrams along the top HBE for the displacement-control and force-control analyses did not reveal a significant difference. Both approaches gave similar results, globally (load-displacement curves) and locally (magnitude and shape of moment and axial force diagrams). Therefore, because the analysis using displacement control was found to achieve a better performance in terms of convergence, it was eventually used for all the finite-element model final analyses.

### Inclination Angle Analysis of SW11 and Deformation of the Top Beam

Fig. 10 shows the overall trend in the variation of the inclination angle as a function of drift for SW11, which is quite similar to the

inclination angle curve shape of Model B observed in Fig. 6, but with values generally higher than those of Model B. For example, for the right column, results fluctuate noticeably for drifts lower than 2% drift, but remain higher than 50°; at 6% drift, the inclination angle reaches 56° in SW11 compared with 50° in Model B. For web plate and beams, the average inclination angles of SW11 reach up to approximately 52° for the web plate and 42° for the beams at 6% drift, compared with the 45° for web plate and 37° for the beams in Model B. The observed fluctuations in the beam results at lower drifts were deemed to result from the deflections of HBE.

To study the cause of the aforementioned fluctuations in results at lower drifts, a few critical drifts for response in the results obtained with the *LS-DYNA* model were first determined and analyzed. In view of symmetry, only results for the top beam are discussed in this study. Von Mises stress contours of Model SW11 for each selected drifts are shown in Fig. 11. These drifts correspond to the development of web yielding and plastic hinging at the right and left ends of the HBE, at around 0.2, 0.9, and 2%, respectively. The shear deformation was found to be non-negligible in the HBE of real SPSWs.

In addition, the principal stress vectors along the boundary elements and in the web plate at 2% drift were obtained from the *LS-DYNA* and plotted in Fig. 12. For clarity in presenting the results, the numerical values shown along the top HBE and left VBE in Fig. 12 are the calculated inclination angles for the shell elements taken at an interval of five elements along the boundary frame. This illustrates that inclination angles along the boundary elements, in this case, vary by as much as 19° along the HBE (from 30.3° to 49.5°) and 8° along the VBE (from 48.3° to 56.0°).

### Optimum Constant Angle for Real SPSW Design

#### Combined Moment–Axial Force Demand Ratio

Because the boundary elements are subjected to combined axial and flexural loading, moment–axial force interaction is considered in their design. To compare the forces obtained from the finite-element analyses with those calculated using constant angle models, it is necessary to perform that comparison considering both the effect of axial and flexural demands. This comparison was done using the following relationship:

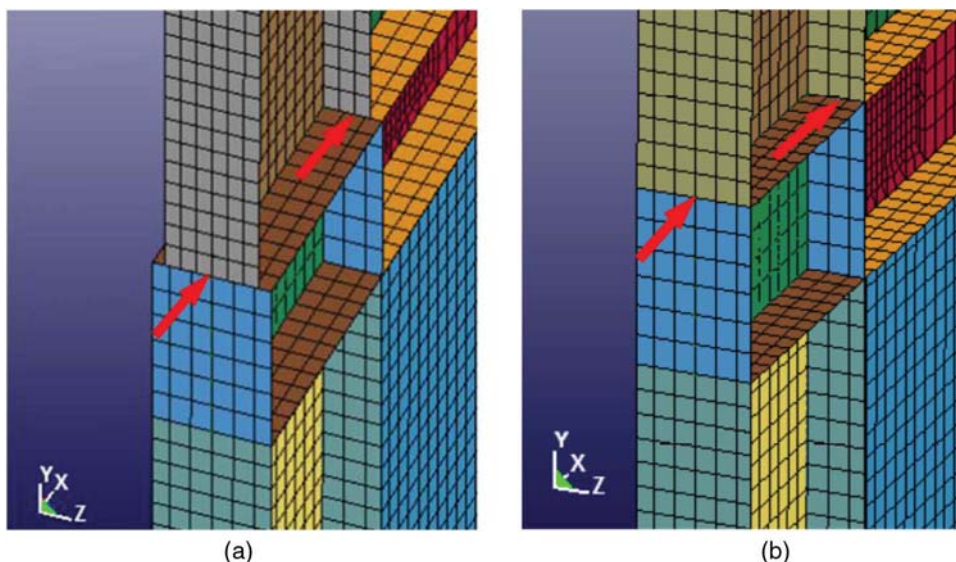
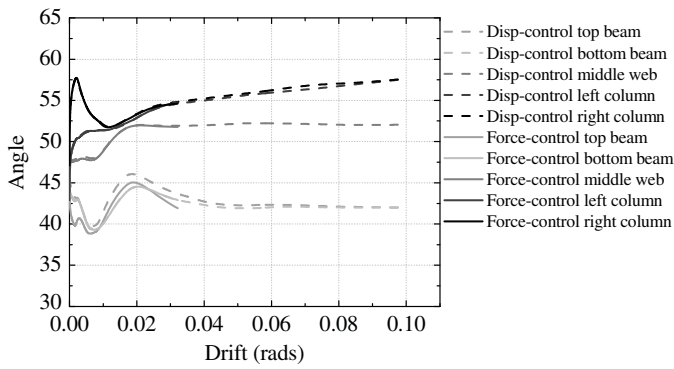


Fig. 9. Section conversion applied for 3-story SPSWs: (a) before section conversion; (b) after section conversion



**Fig. 10.** Inclusion angle comparison for SW11 between force and displacement control

$$\frac{M_u}{M_{u-\alpha}} + \frac{P_u}{P_{u-\alpha}} \leq 2 \quad (1)$$

where  $M_u$  and  $P_u$  = moment and axial demands obtained from the *LS-DYNA*; and  $M_{u-\alpha}$  and  $P_{u-\alpha}$  = moment and axial demands calculated with 35, 40, 45, and 50°, respectively, assuming that the

columns and beams are rigidly framed and infinitely rigid (giving uniform forces applied at uniform angles along the VBEs and HBEs). For safety, the force demands calculated using a constant angle should not be less than those obtained from *LS-DYNA*. Ideally, the ratios of  $M_u/M_{u-\alpha}$  and  $P_u/P_{u-\alpha}$  should be less than or equal to 1, and their sum should be less than or equal to 2, but an acceptable solution could be also obtained if one of those two ratios is greater than one, provided that the sum is less than 2. A comparison of demands using actual interaction diagrams would also be possible, but the preceding approach proposed more explicitly illustrates the discrepancies in flexural and axial demands and how an underestimated demand for one can compensate for an overestimated demand for another.

### Parametric Study of Inclusion Angle for Varying Aspect Ratios and Numbers of Stories

The inclusion angle curves for four real SPSWs are plotted in Fig. 13 in terms of different locations of shell element groups. Floor-by-floor comparison of results was accomplished for SPSWs having aspect ratios of 1 and 2, represented by the solid lines and dashed lines, respectively. The aspect ratio has an impact on the beams and columns of 3-story SPSWs. Fig. 13(a) shows that the inclination angle of top beams under varying aspect ratios generally have a

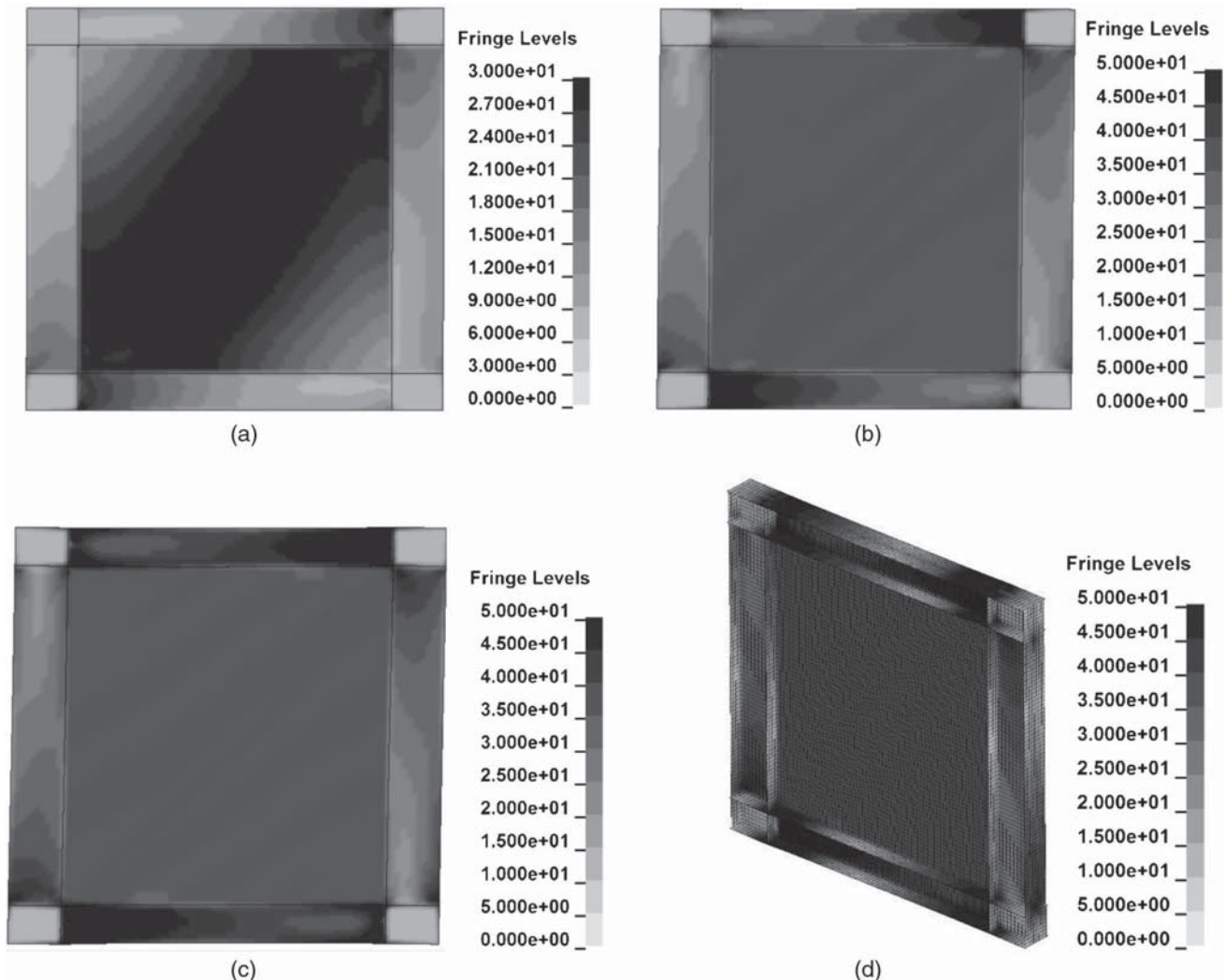


**Fig. 11.** Von-Mises stress contours of Model SW11 at three critical drifts: (a) 0.2%; (b) 0.9%; (c) 2.0%; (d) 3D view at 2.0%



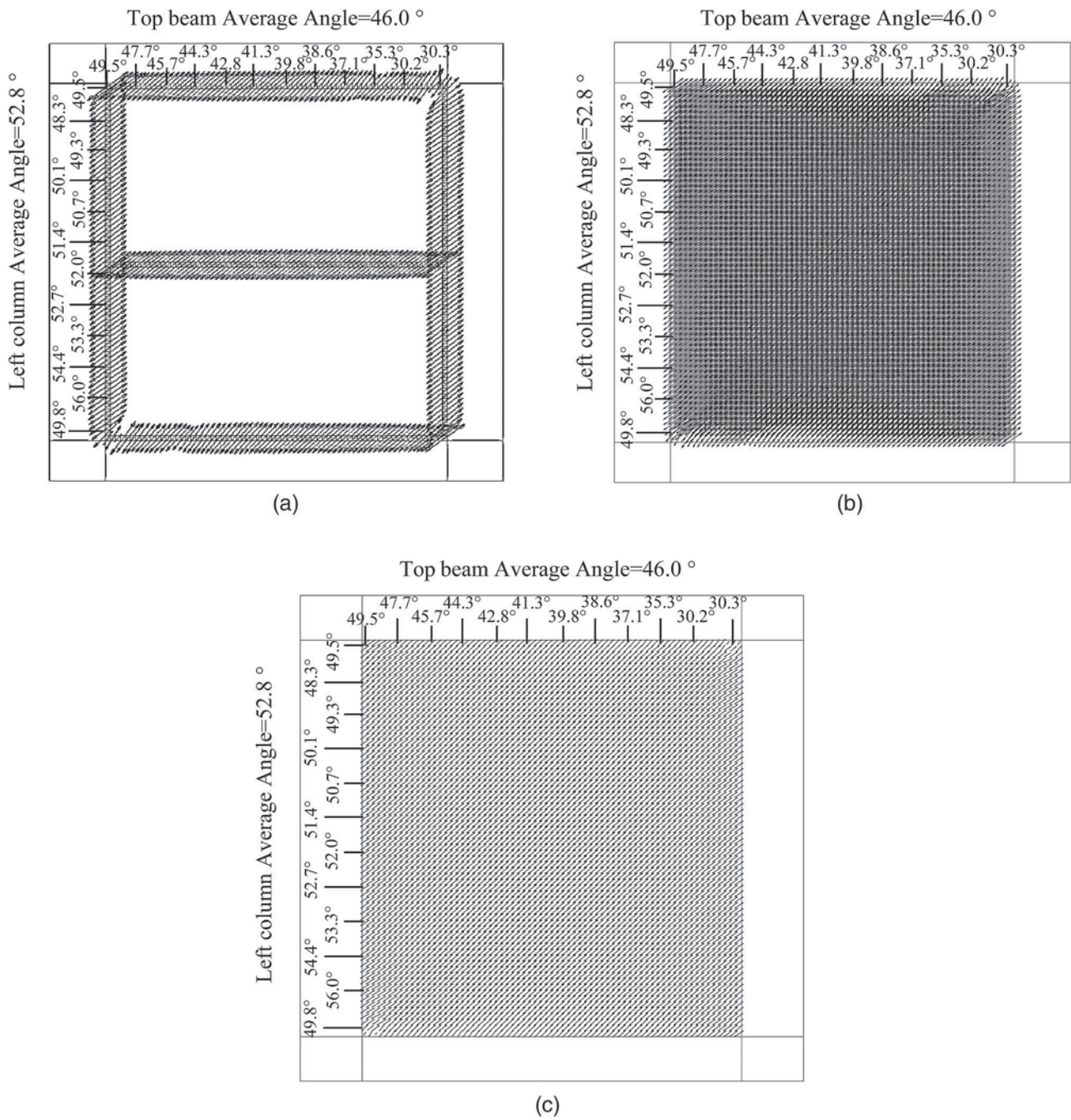


**Fig. 12.** Principal stress vectors of SW11 at 2% drift and different arrow scale factors: (a) 0.1; (b) 0.5; (c) 0.2

difference of approximately 4°; Fig. 13(c) shows that the greater the aspect ratio, the more serious the fluctuation in results obtained for the left columns. Fig. 13(e) shows that the aspect ratio also has an influence on the middle web, taking 1-story SPSWs for example, with a maximum difference of 10° before 2% drift, and 3° for larger drifts.

Regarding the number of stories, the variations on inclination angle for 1-story SPSWs were also compared with those for each floor of the corresponding 3-story SPSWs having identical aspect ratios. Fig. 13 shows that the curves for the columns of 1-story SPSW are significantly different from those for the first floor of the corresponding 3-story SPSW, with up to a 10° difference. However, the magnitude of the differences decreased when compared with the higher floor of 3-story SPSW. As for the top and bottom beams, the curves obtained from the SPSWs with an aspect ratio of

1 show that results for the 1-story SPSW do not match those on any of the floors of the corresponding 3-story SPSW, with a maximum difference of approximately 7° after 2% drift. For the SPSWs with an aspect ratio of 2, this difference is significantly reduced to approximately 3°, and the lower floor matches better with the corresponding 1-story SPSW than the higher floors. Similar observation can be made for the middle web.

Plotted in Fig. 14 are the combined moment–axial force demand ratios of each constant angle considered for the top beam and left column. In terms of aspect ratios, results obtained for the top beam of 1-story SPSWs (filled and open circles) are typically either conservative or nonconservative, namely, either less than 2 when using the constant angle from 35 to 45° or greater than 2 when using the constant angle of 50°. Because the same observation can be

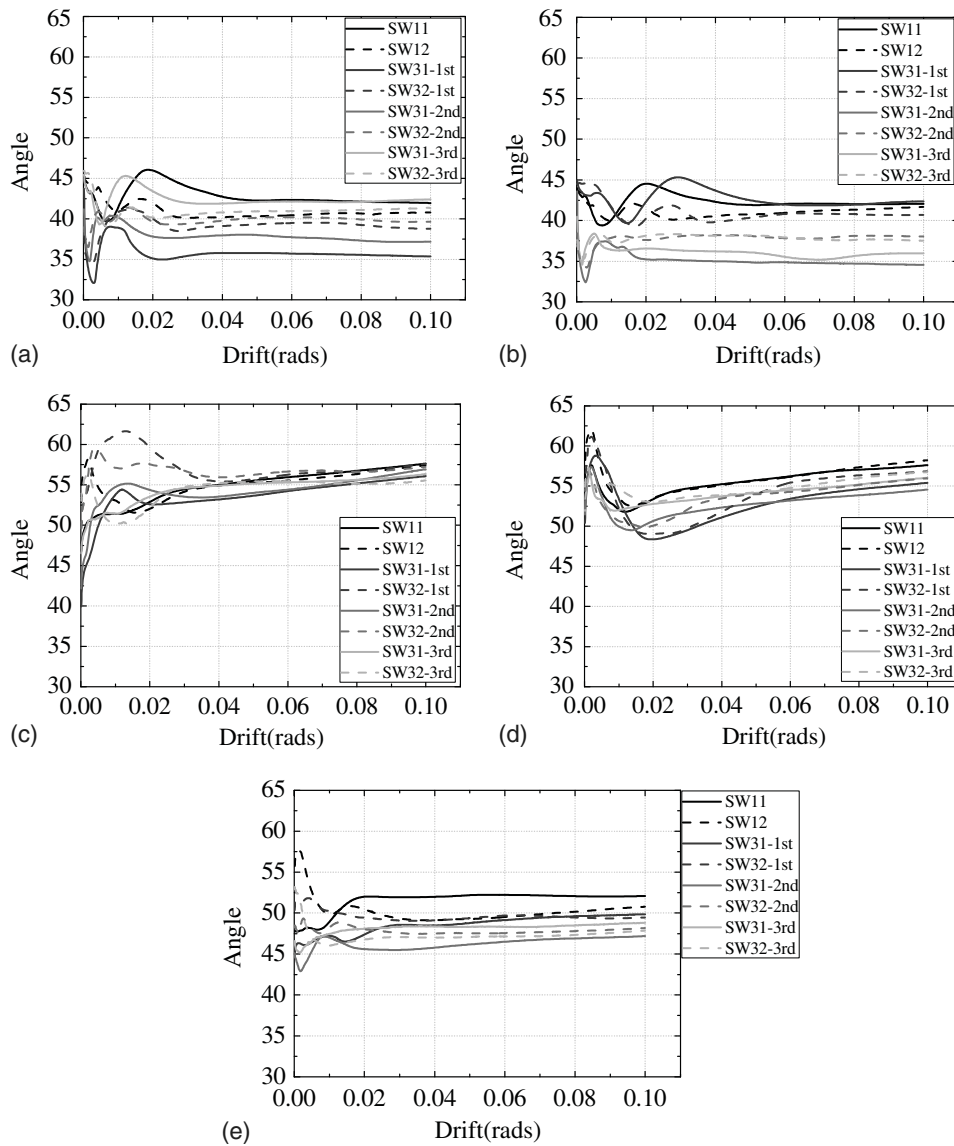


**Fig. 13.** Inclination angle variation for all real SPSWs: (a) top beam; (b) bottom beam; (c) left column; (d) right column; (e) middle web

made for the left column of the 1-story SPSW, the results indicate that the aspect ratio has an insignificant effect on the conservatism of results when constant angles are considered in the design of single-story SPSWs. Regarding the results for the 3-story SPSWs, the results for the top beam using the constant angle of 35, 40, and those for the left column using 50° are always conservative. However, in the case of 45°, changing the aspect ratio changes the level of conservatism of the results obtained from both the top beams and left columns of the second and the third floor of tall SPSWs.

In terms of number of stories, in the case of using a constant angle of 45°, changing the number of stories from one (circles) to three (other symbols) would change the combined moment–axial force demand ratio for the top beams from being conservative to nonconservative, as well as change those for the left columns from being nonconservative to conservative.

### Inclination Angle for Boundary Element Design

Based on the preceding analyses, the inclination angle of the diagonal tension field action along the top beam, along the left column,

and across the middle of the web usually varies from 35° to 45°, 45° to 65°, and 45° to 55°, respectively. These ranges are higher than the corresponding inclination angle ranges for the previous three *LS-DYNA* models, in which a 2D *LS-DYNA* model was used without considering the plastic hinge on the HBEs.

The combined moment–axial force demand analyses resulting for all the analyses conducted as part of this study point to similar conclusions related to the conservatism of using specific constant angles for SPSW design. Generally, it would always be conservative to use a constant angle of 35° and 40° for HBE design and 50° for VBE design. Using a constant angle of 50° for HBE design could be nonconservative by up to 18%, whereas using constant angles of 35° and 40° for VBE design could be nonconservative by up to 38 and 14%, respectively (data are not provided in this paper). However, using different inclination angles for HBEs and VBEs is not practical for design, and it is desirable to use a single constant angle for the design of all structural elements that constitute a SPSW.

The results obtained for both HBE and VBE using a constant angle of 45° are sometimes conservative, sometimes

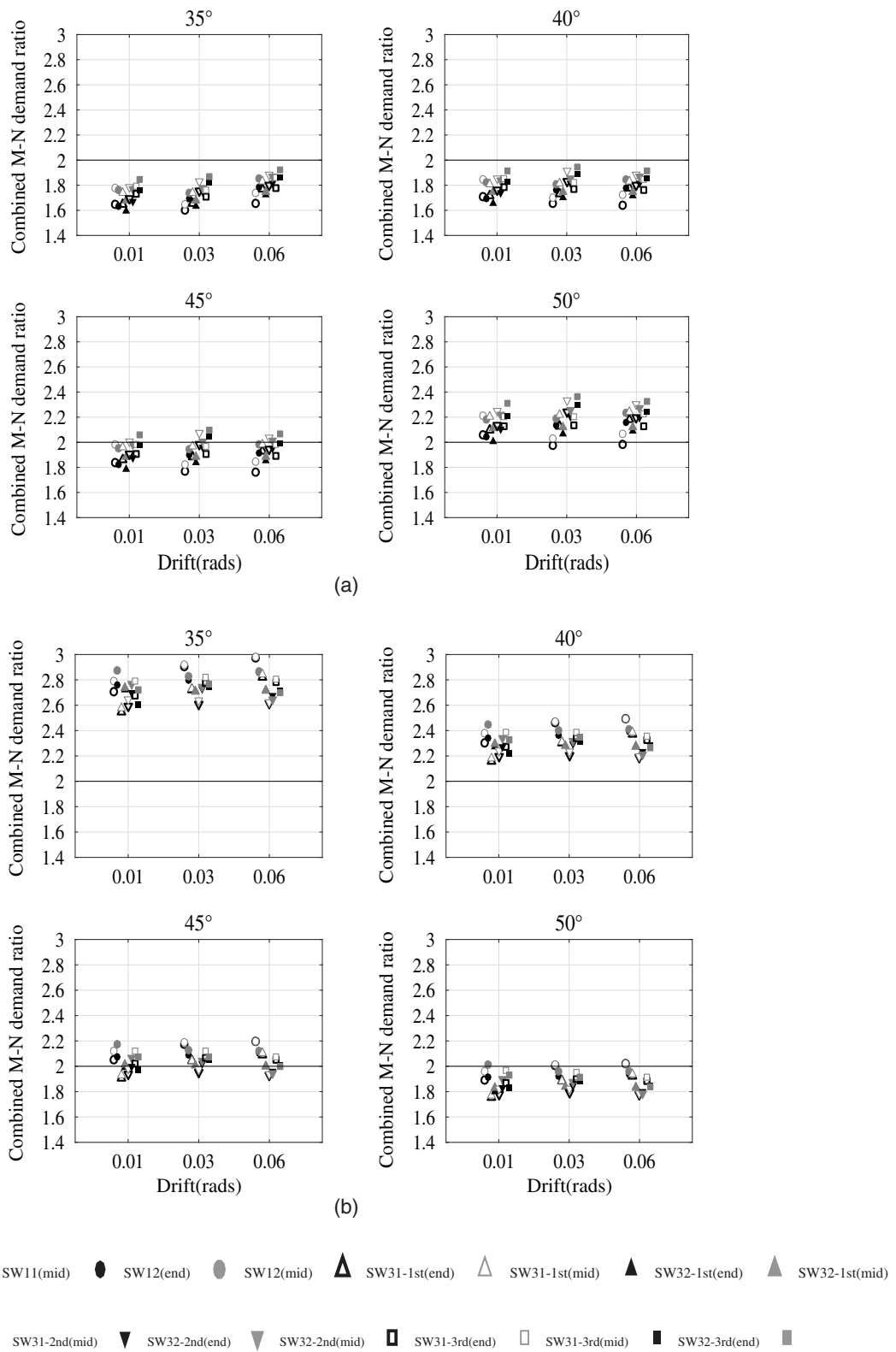


**Fig. 14.** Comparison on combined moment–axial force demand ratios: (a) top beam; (b) left column

nonconservative, and vary from case to case. Table 3 presents a summary of the maximum results obtained for HBEs and VBEs from the preceding case studies when compared with a constant angle of 45°. The ratios greater than the value of 2 are deemed non-conservative and highlighted in bold. Results in this table indicate

that the maximum combined moment–axial force demand ratio was obtained for the case with aspect ratio of 1 (not exceeding the value of 2 by more than 10%). On that basis, the constant angle of 45° is deemed to be the best constant angle to use if desiring to simplify the design process by using a single angle.

**Table 3.** Classification of Boundary Elements With Respect To Conservatism Using the Constant Angle of 45°

SPW	Story	Aspect ratio of 1		Aspect ratio of 2	
		Top beam	Left column	Top beam	Left column
1-story		1.980	<b>2.197</b>	1.984	<b>2.176</b>
3-story	3	1.982	<b>2.123</b>	<b>2.098</b>	<b>2.078</b>
	2	<b>2.071</b>	1.983	<b>2.011</b>	<b>2.067</b>
	1	1.982	<b>2.102</b>	1.886	<b>2.012</b>

Note: The normal text is conservative, whereas the bold text is nonconservative.

### Inclination Angle for Web Plate Design

The web plate is the primary component of SPSW resisting the story shear force. Seismic provisions for structural steel buildings (AISC 2010) stipulates that the design shear strength of the web plate shall be determined as follows:

$$V_n = 0.42F_{yt_w}L_{cf} \sin 2\alpha \quad (2)$$

where  $L_{cf}$  = clear distance between column flanges.

As indicated in Fig. 13(e), the inclination angle of the diagonal tension field action across the middle of the web usually varies from 45 to 55° for real SPSWs. To investigate the influence of inclination angle for the web plate design, the demands in cases SW11 and SW31-2nd floor are compared; these cases are chosen because they respectively represent the cases having the highest and lowest inclination angles. Fig. 15 plots the shear stress distribution obtained from the *LS-DYNA* analyses for each element in the group of web plate at three considered drifts, compared with the design stresses calculated using 35°, 40°, and 45° [results for 55° and 50° are identical to those for 40° and 35°, respectively, because of  $\sin 2\alpha$  in Eq. (2)]. The stress distributions are compared with the design stresses considering various design-specified yield stress values.

The shear stress distributions of SW11 at the three considered drifts and those of SW31-2nd floor at 1% drift are close to

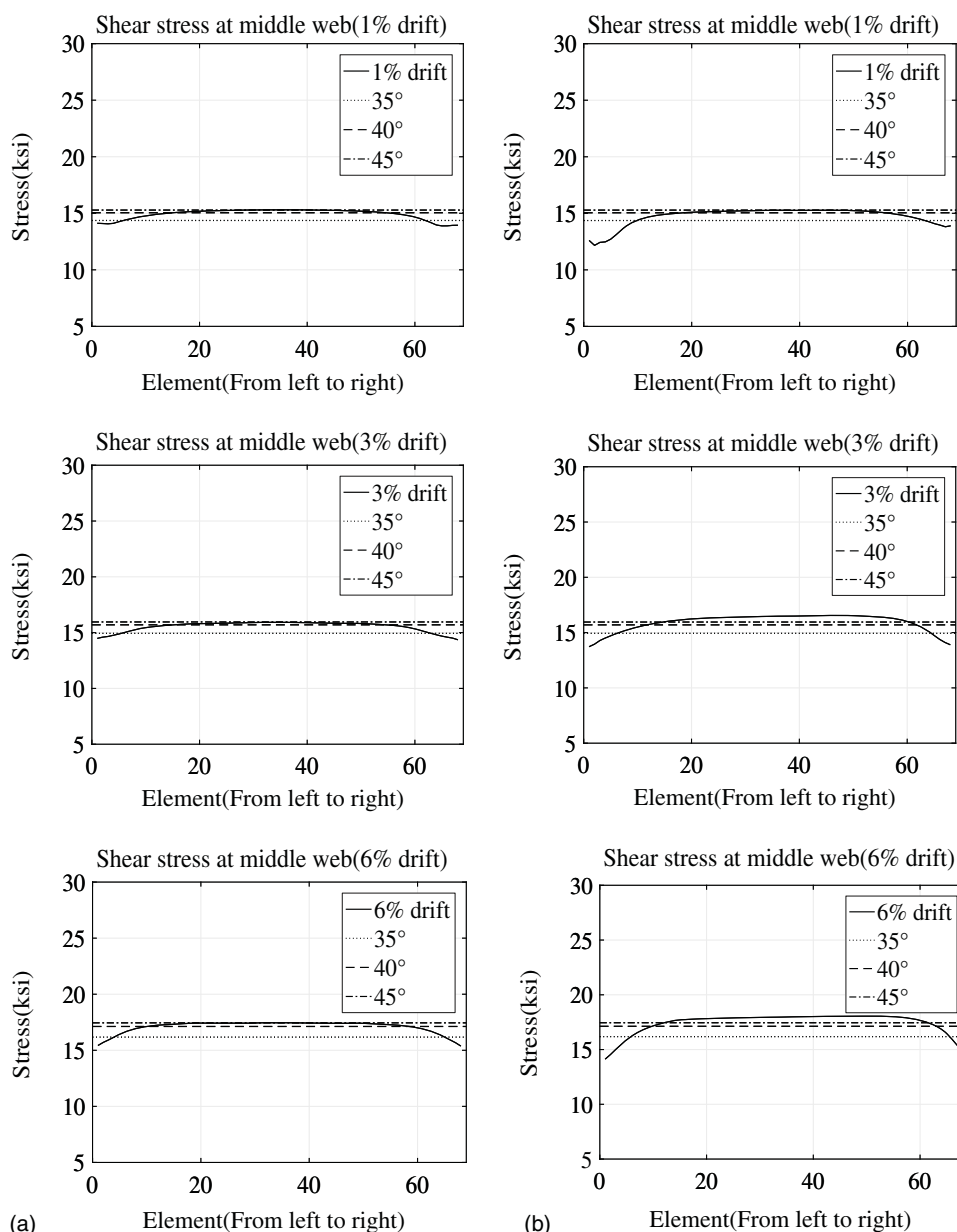


**Fig. 15.** Comparison on shear stress of web plate shell elements (middle web): (a) SW11; (b) SW31-2nd floor

the design stresses, whereas the shear stresses at 3 and 6% drift of SW31-2nd floor are slightly higher than the design stress at midspan, with a difference of approximately 6.9 MPa (1 ksi).

These observations confirm that orienting the design stresses in the web at angles ranging from 35° to 55° is of minimal consequence because of the  $\sin 2\alpha$  in Eq. (2). Therefore, both inclination angles of 40° (currently in AISC 2010) and 45° (proposed in this study) are conservative for the web plate design.

## Conclusion

The variation in the inclination angle of diagonal tension field action observed in the seven models considered (i.e., the validated model, Models A and B, SW11, SW12, SW31, and SW32) indicate that significantly different average inclination angles occur at different locations of the web plate, and each of those inclination angles varies as a function of drifts, panel aspect ratios, and number of stories. For real SPSWs designed per AISC (2010), the inclination angle for the top beam, left column, and web plate usually varies from 35° to 45°, 45° to 65°, and 45° to 55°, respectively.

Variations in inclination angles were compared with respect to different SPSW panel aspect ratios and number of stories. The aspect ratio has a noticeable impact on the inclination angle for the middle web of 1-story SPSW, with a maximum difference of 10° before 2% drift, and 3° for larger drifts. It also influences the curves for the columns of the tall SPSWs by inducing serious fluctuations as the aspect ratio increases. The inclination angle for the top beams of tall SPSWs under varying aspect ratios generally have a difference within 4°.

In addition, the number of stories influences all curves. For the columns, the curves for the 1-story SPSW differ from those for the first floor of the corresponding 3-story SPSW up to 10°. However, these differences decreased when compared with the higher floor of a 3-story SPSW. For the beams, the curves obtained from the 1-story SPSWs seldom match those on the floors of the corresponding 3-story, with a maximum difference of approximately 7° after 2% drift. Similar observation can be made for the middle web.

With respect to the combined moment–axial force demands, the analyses conducted indicated that changing the aspect ratio of the walls did not change the level of conservatism in the results obtained when comparing results for the same constant angles considered in respective 1-story SPSWs, but that it would change the level of conservatism for the results obtained in 3-story SPSWs, most significantly when using a constant angle of 45°. The number of stories also impacted the conservatism of the results obtained using the constant angle of 45°, because the combined moment–axial force demand ratio of the top beams changed from being conservative to nonconservative as the number of stories increased, and those for the left columns changed from being nonconservative to conservative as the number of stories increased.

In summary, it was always conservative to use 35° and 40° for HBE and 50° for VBE design. Using a constant angle of 50° for HBE design could be nonconservative by up to 18%, whereas using constant angles of 35° and 40° for VBE design could be nonconservative by up to 38 and 14%, respectively. However, using different inclination angles for HBEs and VBEs is not practical for design, and it is desirable to use a single constant angle for the design of all structural elements that constitute a SPSW. Using the constant angle of 45° would yield a good compromise for both

HBEs and VBEs design if it is desirable to simplify the design process by using a single angle. In addition, the demand of the web plate is not sensitive to the variation of inclination angle. Consequently, the single angle of 45° is recommended for the design of the entire SPSW.

## Future Research

This research considered seven SPSWs as case studies using finite-element analysis. Four of these SPSWs had boundary elements designed in compliance with AISC (2010), allowing the consideration of two panel aspect ratios and two different of numbers of stories. More case studies could be conducted in the future to extend the number of SPSWs considered. Such future parametric studies would be useful to further investigate and verify the trends in variation of the inclination angle as a function of aspect ratio and number of stories.

Furthermore, all current evidence in this study was used to determine the value of constant angle by using either monotonic loading or cyclic analysis scenarios. This was done because SPSW web plates are typically slender and behave in a tension-only manner, typically not re-engaging in subsequent cycles of displacement before reaching anew the maximum drift previously attained during a displacement history. However, future studies could investigate whether results obtained would change significantly under actual seismic loading scenarios, possibly owing to the small compression capacity that can develop in parts of the web plates (near the corners or in particularly thicker plates).

## References

- ABAQUS 6.9 [Computer software]. Dassault Systèmes Simulia, Providence, RI.
- AISC. (2010). “Seismic provisions for structural steel buildings.” *ANSI/AISC 341-10*, Chicago.
- Choi, I. R., and Park, H. G. (2009). “Steel plate shear walls with various infill plate designs.” *J. Struct. Eng.*, 10.1061/(ASCE)0733-9445(2009)135:7(785), 785–796.
- Dastfan, M., and Driver, R. G. (2008). “Flexural stiffness limits for frame members of steel plate shear wall systems.” *Proc., Annual Stability Conf.*, Structural Stability Research Council, Nashville, TN, 321–334.
- Driver, R. G., Kulak, G. L., Kennedy, D. J. L., and Elwi, A. E. (1997). “Seismic behavior of steel plate shear walls.” *Structural Engineering Rep. No. 215*, Univ. of Alberta, Edmonton, AB, Canada.
- Elgaaly, M., Caccese, V., and Du, C. (1993). “Post-buckling behavior of steel plate shear walls under cyclic loads.” *J. Struct. Eng.*, 10.1061/(ASCE)0733-9445(1993)119:2(588), 588–605.
- Fu, Y., Wang, F., and Bruneau, M. (2017). “Diagonal tension field inclination angle in steel plate shear wall.” *Technical Rep. MCEER-17-0001*, Multidisciplinary Center for Earthquake Engineering Research, State Univ. of New York at Buffalo, NY.
- Kharrazi, M. H. K. (2005). “Rational method for analysis and design of steel plate walls.” Ph.D. thesis, Univ. of British Columbia, Vancouver, BC, Canada.
- LS-DYNA v971 [Computer software]. Livermore Software Technology Corporation, Livermore, CA.
- Lubell, A. S. (1997). “Performance of unstiffened steel plate shear walls under cyclic quasi-static loading.” Master’s thesis, Univ. of British Columbia, Vancouver, BC, Canada.
- Purba, R., and Bruneau, M. (2010). “Impact of horizontal boundary elements design on seismic behavior of steel plate shear walls.” *Technical Rep. MCEER-10-0007*, Multidisciplinary Center for Earthquake

- Engineering Research, State Univ. of New York, Buffalo, Buffalo, NY.
- Rezai, M. (1999). "Seismic behavior of steel plate shear walls by shake table testing." Ph.D. thesis, Univ. of British Columbia, Vancouver, BC, Canada.
- Timler, P. A., and Kulak, G. L. (1983). "Experimental study of steel plate shear walls." *Structural Engineering Rep. No. 114*, Univ. of Alberta, Edmonton, AB, Canada.
- Webster, D. J. (2013). "The inelastic seismic response of steel plate shear wall web plates and their interaction with the vertical boundary members." Ph.D. thesis, Univ. of Washington, Seattle.
- Webster, D. J., Berman, J. W., and Lowes, L. N. (2014). "Experimental investigation of SPSW web plate stress field development and vertical boundary element demand." *J. Struct. Eng.*, [10.1061/\(ASCE\)ST.1943-541X.0000989](https://doi.org/10.1061/(ASCE)ST.1943-541X.0000989), 04014011.